Heme catalyzes tyrosine 385 nitration and inactivation of prostaglandin H_2 synthase-1 by peroxynitrite

Ruba S. Deeb,[1,*] Gang Hao,[†] Steven S. Gross,[*,†] Muriel Lainé,[*] Ju Hua Qiu,[*] Brad Resnick,[*] Elisar J. Barbar,[§] David P. Hajjar,[*] and Rita K. Upmacis[*]

Department of Pathology and Laboratory Medicine, Center of Vascular Biology,* and Department of Pharmacology,† Weill Medical College of Cornell University, New York, NY 10021; and Department of Biochemistry and Biophysics,§ Oregon State University, Corvallis, OR 97331

Abstract **The mechanism by which the inflammatory enzyme prostaglandin H_2 synthase-1 (PGHS-1) deactivates remains undefined. This study aimed to determine the stabilizing parameters of PGHS-1 and identify factors leading to deactivation by nitric oxide species (NO_x). Purified PGHS-1 was stabilized when solubilized in β-octylglucoside (rather than Tween-20 or CHAPS) and when reconstituted with hemin chloride (rather than hematin). Peroxynitrite ($ONOO^-$) activated the peroxidase site of PGHS-1 independently of the cyclooxygenase site. After $ONOO^-$ exposure, holoPGHS-1 could not metabolize arachidonic acid and was structurally compromised, whereas apoPGHS-1 retained full activity once reconstituted with heme. After incubation of holoPGHS-1 with $ONOO^-$, heme absorbance was diminished but to a lesser extent than the loss in enzymatic function, suggesting the contribution of more than one process to enzyme inactivation. Hydroperoxide scavengers improved enzyme activity, whereas hydroxyl radical scavengers provided no protection from the effects of $ONOO^-$. Mass spectral analyses revealed that tyrosine 385 (Tyr 385) is a target for nitration by $ONOO^-$ only when heme is present. Multimer formation was also observed and required heme but could be attenuated by arachidonic acid substrate. We conclude that the heme plays a role in catalyzing Tyr 385 nitration by $ONOO^-$ and the demise of PGHS-1.**—Deeb, R. S., G. Hao, S. S. Gross, M. Lainé, J. H. Qiu, B. Resnick, E. J. Barbar, D. P. Hajjar, and R. K. Upmacis. **Heme catalyzes tyrosine 385 nitration and inactivation of prostaglandin H_2 synthase-1 by peroxynitrite.** ***J. Lipid Res.*** **2006.** 47: **898–911.**

Supplementary key words cyclooxygenase • eicosanoids • heme reconstitution • peroxidase activity • proteolysis • mass spectrometry

Eicosanoids such as the prostaglandins, thromboxanes, and leukotrienes, which are formed from arachidonic acid metabolism, regulate vascular tone and platelet aggregation (1). Alterations in eicosanoid metabolism occur during the pathogenesis of inflammatory diseases (2), but the mechanisms are not well established.

Manuscript received 24 August 2005 and in revised form 20 January 2006.

Published, JLR Papers in Press, February 9, 2006.
DOI 10.1194/jlr.M500384-JLR200

Eicosanoid biosynthesis is initiated by prostaglandin H_2 synthase-1 (PGHS-1) and PGHS-2. Although similar in structure, PGHS-1 and PGHS-2 have distinct roles. PGHS-1 is constitutively expressed in most tissues and has homeostatic functions, whereas PGHS-2 is inducible and found mainly at sites of inflammation (3, 4). PGHS enzymes are glycosylated membrane proteins that are dimeric. Each dimer consists of identical monomers of 70 kDa and contains three domains: an epidermal growth factor domain, a membrane binding domain, and a catalytic domain comprising the cyclooxygenase and heme-containing peroxidase active sites (5). PGHS metabolizes the substrate arachidonic acid to prostaglandin G_2 and prostaglandin H_2 in two sequential reactions. The cyclooxygenase site binds arachidonic acid and converts it to prostaglandin G_2, which is then reduced to the cyclic endoperoxide prostaglandin H_2 by the heme-containing peroxidase site (6–8). The cyclooxygenase site is the target for nonsteroidal anti-inflammatory drugs, such as aspirin and ibuprofen, which interfere with the binding of arachidonic acid (7). During catalysis, the enzyme undergoes irreversible self-inactivation (9). The generation of a ferryl-oxo porphyrin intermediate, followed by tyrosine radical formation at tyrosine 385 (Tyr 385), is thought to be essential for activation/inactivation (6, 10). Others have suggested that a cluster of aromatic amino acids in the vicinity of the heme group in addition to Tyr 385 can form radicals involved in enzyme catalysis and inactivation (11). Recently, it was shown that the process of PGHS-1 oxidant-driven inactivation is altered by inhibitor

Abbreviations: $C_{10}M$, *N*-decyl-β-D-maltopyranoside; DEDTC, diethyldithiocarbamate; ε, extinction coefficient; EtOH, ethanol; KI, potassium iodide; L-NAME, N^G-nitro-L-arginine methyl ester; MALDI-TOF, matrix-assisted laser desorption/ionization time-of-flight; nLC-MS/MS, nanoflow liquid chromatography-tandem mass spectrometry; NO_x, nitric oxide species; NOC-7, 1-hydroxy-2-oxo-3-(*N*-methyl-aminopropyl)-3-methyl-1-triazene; βOG, *N*-octyl-β-D-glucopyranoside; $^{\bullet}OH$, hydroxyl radical; $ONOO^-$, peroxynitrite; PGHS-1, prostaglandin H_2 synthase-1; SIN-1, 3-morpholinosydnonimine hydrochloride; TMPD, *N,N,N′,N′*-tetramethylphenylenediamine; TNM, tetranitromethane; Tyr 385, tyrosine 385; UV-Vis, ultraviolet-visible.

[1] To whom correspondence should be addressed.
e-mail: rsdeeb@med.cornell.edu

binding to the cyclooxygenase channel, which likely leads to radical formation at a site different from Tyr 385 (12). Key unresolved questions include the mechanism(s) of PGHS suicide inactivation, the factors that contribute to its deactivation, and the involvement of enzyme modification in these processes.

Evidence suggests that nitric oxide species (NO_x) modulate PGHS activity and eicosanoid production under physiological conditions (13, 14). Investigations of the direct effect of NO and NO-derived species on purified PGHS-1 enzyme activity have been controversial, with reports of activation (15–18) as well as inhibition (19). The complexity of NO chemistry, which results in the formation of various NO species such as nitrite (NO_2^-), nitrate (NO_3^-), nitrosonium ion (NO^+), nitroxyl anion (NO^-), peroxynitrite ($ONOO^-$), and nitrosoperoxocarbonate (ONO_2CO2^-), can contribute to the variable actions (20–22). Thus, although one particular form of NO_x may stimulate PGHS-1 activity, another form inhibits. Our studies indicate that one particular NO_x, $ONOO^-$, has several modes of action on PGHS-1. First, $ONOO^-$ directly activates PGHS-1 by serving as a peroxide substrate, leading to heme oxidation (15). Second, $ONOO^-$ indirectly affects eicosanoid biosynthesis via modification of signaling processes that are upstream of PGHS, thus controlling arachidonic acid availability to the enzyme (23). Finally, $ONOO^-$ nitrates purified PGHS-1 in the absence of arachidonate (24, 25), and PGHS-1 is nitrated in human atherosclerotic lesions (24). It has been shown that tetranitromethane (TNM) and $ONOO^-$ nitrate two to three Tyr residues per PGHS-1 monomer, resulting in the loss of enzyme function (24–26, 28). It is likely that one of the Tyr residues nitrated is Tyr 385, and in fact, it has been shown that NO from NOC-9 [1-Hydroxy-2-oxo-3-(N-methyl-6-aminohexyl)-3-methyl-1-triazene] (27) and TNM (28) lead to Tyr 385 nitration in PGHS-1.

In this study, we investigated the role of the peroxidase heme on NO_x-induced modification and loss of function in PGHS-1. In particular, the NO_x that we used in our studies included $ONOO^-$, 3-morpholinosydnonimine hydrochloride (SIN-1; which produces low levels of superoxide and NO that form $ONOO^-$), 1-hydroxy-2-oxo-3-(*N*-methyl-aminopropyl)-3-methyl-1-triazene (NOC-7; which produces NO), NO_2^-, and NO_3^-. We demonstrate that the active heme center of PGHS-1 regulates $ONOO^-$-induced modification and loss of enzyme reactivity. These modifications are manifested as changes in PGHS-1 solvent accessibility and heme absorption characteristics, Tyr nitration, and multimer formation. We also show that in the absence of heme, PGHS-1 Tyr nitration occurs, but not at Tyr 385 and with no impact on the ability of PGHS-1 to reconstitute heme and metabolize arachidonic acid.

MATERIALS AND METHODS

Ram seminal vesicles were obtained from Pel Freeze. Heptaoxyethylene decyl ether, diethyldithiocarbamate (DEDTC), hemin chloride (hemin), hematin, GSH, GSH peroxidase, sodium nitrite, sodium nitrate, TNM, CHAPS, Tween-20, and LysC endoproteinase were obtained from Sigma-Aldrich (minimum 95% purity; HPLC grade). NOC-7 was purchased from Alexis Biochemicals. Arachidonic acid (99% purity, by capillary GC) was obtained from Sigma-Aldrich, solubilized in ethanol (EtOH), and stored in aliquots (168 mM) at −80°C. *N,N,N′,N′*-tetramethylphenylenediamine (TMPD), also from Sigma-Aldrich, was prepared freshly for each experiment as a 1 mg/ml stock solution. Aspirin, SIN-1, and N^G-nitro-L-arginine methyl ester (L-NAME) were purchased from Cayman Chemicals. *N*-Decyl-β-D-maltopyranoside ($C_{10}M$) and *N*-octyl-β-D-glucopyranoside (βOG) were purchased from Anatrace. Sodium peroxynitrite (170–200 mM in 4.7% sodium hydroxide) was obtained from Calbiochem. Monoclonal 3-nitrotyrosine antibody (clone 1A6) was obtained from Upstate Biotechnology. Monoclonal PGHS-1 antibody was obtained from Cayman. Anti-mouse horseradish peroxidase-conjugated IgG and ECL Plus reagents were obtained from GE Healthcare. All materials for SDS-PAGE and Western blotting were obtained from Bio-Rad Laboratories. Fast-flow DEAE-Sepharose and S-200 and S-300 beads were purchased from GE Healthcare.

Isolation and purification of PGHS-1 from ram seminal vesicles

PGHS-1 solubilized in Tween-20 was purified from ram seminal vesicles (300 g) as described previously by Van der Ouderaa et al. (29). When using CHAPS or βOG, purified PGHS-1 was obtained by the procedure described by Malkowski et al. (30), although we implemented modifications described below to enable purification by regular-flow liquid chromatography. Concentrations of detergents used in the purifications were chosen based on the published literature (29, 30). Levels of detergent used in our experiments are the residual amounts present that result from the purification process. For PGHS-1 solubilized in CHAPS or βOG, microsomal homogenates obtained in the absence of detergent were extracted with heptaethylene glycol monodecyl ether and $C_{10}M$ and stored at −80°C.

Frozen microsomal extracts (70 ml) were rapidly thawed and loaded on a fast-flow DEAE-Sepharose column (20 cm × 1.5 cm) preequilibrated with wash buffer (10 mM Tris, 10 mM Bis-Tris, 1 mM NaN_3, and 0.15% $C_{10}M$, pH 8.5). **Figure 1A** shows the chromatogram for the elution profile described below. The column was washed with two column volumes (V_0 = 40 ml) of equilibration buffer followed by linear pH gradient I (rate, 2 ml/min) [(40 ml) 10 mM Tris, 10 mM Bis-Tris, 1 mM NaN_3, and 0.15% $C_{10}M$, pH 8.5, to (40 ml) 40 mM Tris, 40 mM Bis-Tris, 20 mM NaCl, 1 mM NaN_3, 0.05 mM EDTA, 0.1 mM DEDTC, and 0.15% $C_{10}M$, pH 6.5]. Note that during the column wash stage, a major protein band (peak a), which has no PGHS-1 activity, eluted off the column (Fig. 1A). Active PGHS-1 eluted from the column with salt gradient II [(40 ml) 40 mM Tris, 40 mM Bis-Tris, 20 mM NaCl, 1 mM NaN_3, 0.05 mM EDTA, 0.1 mM DEDTC, and 0.15% $C_{10}M$, pH 6.5, to (40 ml) 40 mM Tris, 40 mM Bis-Tris, 500 mM NaCl, 1 mM NaN_3, 0.05 mM EDTA, 0.1 mM DEDTC, and 0.15% $C_{10}M$, pH 6.5]. Highly active fractions of ~90% apoPGHS-1 eluted off the column ~30 ml into gradient II, in a sharp and narrow band (Fig. 1A, peak b). Peak b′ represents the fractions absorbing at 412 nm (the Soret band) that are holoPGHS-1 (~10%). The second band to follow (Fig. 1A, peak c) was broader and contained more heme (peak c′) but was significantly less active than peak b fractions. Fractions from peak b were combined, concentrated, and desalted on a S-300 gel filtration column for use in this study.

ApoPGHS-1 was concentrated on Ultra-15 spin concentrators (50 kDa cutoff; Millipore Corp.) to <5 ml. The concentrate was adjusted to 1% (w/v) $C_{10}M$ and loaded on a S-300 column

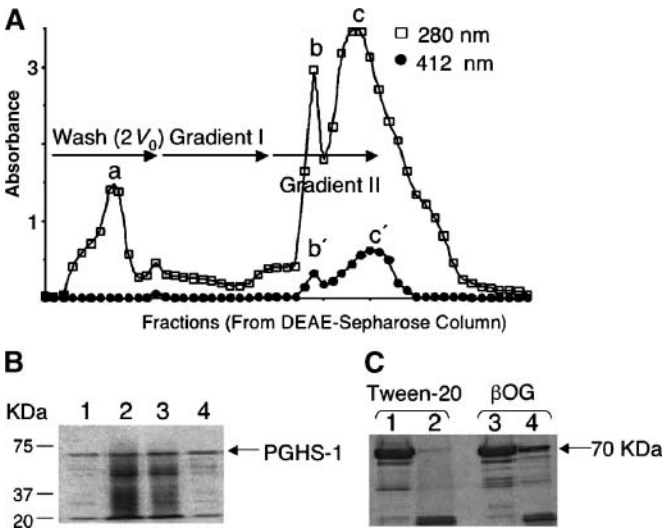

Fig. 1. Purification of ovine prostaglandin H_2 synthase-1 (PGHS-1). A: Elution profiles at 280 nm (open squares) and 412 nm (closed circles) of PGHS-1 fractions from the DEAE-Sepharose column. Individual peaks are described in Materials and Methods. B: SDS-PAGE (10% acrylamide) of PGHS-1 fractions from various stages of the purification. Lane 1, commercially obtained purified PGHS-1 solubilized in Tween-20; lane 2, homogenate from seminal vesicles; lane 3, supernatant from solubilized microsomes in *N*-decyl-β-D-maltopyranoside (C_{10}M); lane 4, column-purified PGHS-1 solubilized in *N*-octyl-β-D-glucopyranoside (βOG). C: SDS-PAGE (10% acrylamide) analysis of the 70 kDa band that remains of holoPGHS-1 (12 mg) solubilized in Tween-20 (lane 2) and in βOG (lane 4) after digestion with LysC endoproteinase (1 unit) for 18 h. Undigested holoPGHS-1 (12 mg) in Tween-20 and βOG are shown in lanes 1 and 3, respectively.

(80 cm × 2.5 cm) preequilibrated with 20 mM Tris, 50 mM NaCl, 1 mM NaN_3, 0.1 mM EDTA, 0.1 mM DEDTC, and 0.15% C_{10}M, pH 8. An active peak with a trailing shoulder eluted off the S-300 column (data not shown). Fractions containing the active peak were pooled, concentrated to 2 ml, and adjusted to either 1% (w/v) βOG or CHAPS. Detergent was exchanged on a S-200 column (80 cm × 2.5 cm) preequilibrated with 100 mM Tris, 5 mM GSH, 5 mM EDTA, 0.3 mM DEDTC, and 0.3% (w/v) βOG or 0.4% (w/v) CHAPS, pH 8.0. A single active peak eluted from the column, and the protein content in each fraction was determined using the Bio-Rad protein assay, measuring absorbance at 595 nm. The use of GSH during the last step removed residual heme from PGHS-1. Purified apoPGHS-1 was then concentrated and exchanged into appropriate buffers without GSH to prevent its interference in the reactions described below. Yields were determined by ultraviolet-visible spectroscopy (described below).

Protein identity and purity were confirmed by Western blot analysis, SDS-PAGE (10% acrylamide), amino acid sequencing, and mass spectrometric analysis of peptide fragments from PGHS-1 digests, as described briefly below. The band corresponding to PGHS-1 was excised from a SDS-PAGE gel, washed, and digested with trypsin, and the peptides were extracted and lyophilized. Molecular mass analysis on the peptide digests from gels was performed by matrix-assisted laser desorption/ionization time-of-flight (MALDI-TOF) mass spectrometry using an Applied Biosystems ABI4700 TOF/TOF mass spectrometer (Applied Biosystems, Inc., Farmingham, MA) with an accelerating voltage of 20 kV. Samples were mixed in a 1:6 ratio with α-cyano-4-hydroxycinnamic acid in 50% acetonitrile and 0.1% triflouroacetic acid. An aliquot of the sample solution (0.5 μl) was applied to the sample plate and air-dried before mass spectral analysis.

MALDI-TOF analysis of free heme from HoloPGHS-1

$ONOO^-$-treated holoPGHS-1 samples were exchanged into detergent-free buffer using Centricon spin filters and mixed in a 1:1 ratio with sinapinic acid solution (10 mg/ml in 50% acetonitrile, 50% water, and 0.1% triflouroacetic acid). Samples were applied to a target plate for MALDI-TOF analysis using a Voyager DE Pro (Applied Biosystems) MALDI-TOF mass spectrometer in reflectron mode.

Liquid chromatography-tandem mass spectrometry analysis of nitrated PGHS-1 and database search

Nanoflow liquid chromatography-tandem mass spectrometry (nLC-MS/MS) was used to identify sites of Tyr nitration in peptides from apoPGHS-1 and holoPGHS-1 treated with $ONOO^-$ and SIN-1. Analyses were performed using an 1100 series LC/MSD XCT plus or an 1100 series LC/MSD XCT ultra ion trap mass spectrometer with a chip cube (Agilent). The mobile phases were 0.1% formic acid in 3% acetonitrile (solvent A) and 0.1% formic acid in 100% acetonitrile (solvent B). ApoPGHS-1 and holoPGHS-1 (8 μM in 13 μl) were each incubated with $ONOO^-$ (1 mM) or SIN-1 (2 mM) for 1 h at room temperature. Proteins were precipitated by adding 2 volumes of acetone, centrifuged, and then resolubilized in ammonium bicarbonate (20 mM, pH 8). After reduction by DTT (10 mM; 30 min at 50°C) and alkylation by iodoacetamide (50 mM; 30 min at ambient temperature), proteins were digested with 1:100 sequencing grade trypsin (Promega):PGHS-1 for 8 h at 37°C. Samples were diluted 100-fold with solvent A, 8 μl of the protein digest was injected onto a 0.3 × 5 mm Zorbax 300SB-C18 enrichment column at a flow rate of 10 μl/min, and peptides were subsequently resolved on a 0.075 × 150 mm Zorbax 300SB-C18 analytical column (3.5 μm particle size) at a flow rate of 0.3 μl/min with a gradient of 10–40% solvent B for 40 min and 40–80% solvent B for 30 min. Mass spectra were acquired in the automated MS/MS mode, in which MS/MS scans were performed on the three most intense ions from each MS scan (acquired at 0.5 s intervals). The MS/MS spectra were used to identify the sites of Tyr nitration in PGHS-1 by a database search using SpectrumMill software (Millennium Pharmaceuticals). The parameters for searching were as follows: minimum matched peak intensity of 50%, precursor mass tolerance of 2.5 Da, and product mass tolerance of 0.7 Da. The program was instructed to account for Tyr nitration when matching peptide fragments to PGHS-1.

Ultraviolet-visible spectroscopy

Ultraviolet-visible (UV-Vis) spectroscopy experiments were performed using a Perkin-Elmer Lambda 20 spectrophotometer. Matching cells [Hellma (Plainview, NY); 1 cm path length, 1 ml or 200 μl volume] were used. For each heme reconstitution experiment, an aliquot of freshly prepared hemin or hematin at the desired concentration was added to a sample cell containing apoPGHS-1, and the absorbance was measured at 412 nm. After each addition, the increase in optical density proportionally reflected the amount of reconstituted holoPGHS-1 ($\epsilon = 1.42 \times 10^5\ M^{-1}cm^{-1}$) (31, 32). Titration was completed when the absorbance remained constant upon further additions of heme (31). The concentration of excess heme was calculated by subtracting the concentration of reconstituted holoPGHS-1 at 412 nm (10 μM) from the total concentration of heme used for each reconstitution. Note that free heme contributes to the spectrum of holoPGHS-1 at 385 nm when present. From the

absorbance spectrum of heme-reconstituted holoPGHS-1 (to a 1:1 molar complex), we calculated a yield of 43 mg (from 300 g of seminal vesicles), which compares well with the yield calculated using the Bio-Rad protein assay (36 mg).

The concentration of $ONOO^-$ used for each experiment was determined by measuring absorbance at 302 nm (ϵ = 1,670 M^{-1} cm^{-1}). For control experiments using decomposed $ONOO^-$, the $ONOO^-$ maximum at 302 nm was completely decayed. Absorbance spectra for the reactions of $ONOO^-$ (250 μM) and NOC-7 (250 and 750 μM) with holoPGHS-1 (10 μM) were monitored between 200 and 700 nm (2, 10, 20, and 60 min) after the addition of NO_x. For each time point, the activity was measured as described below.

Treatment of purified PGHS with NO_x

PGHS-1 reactions with NO_x were conducted in 20 mM HEPES/20 mM NaCl at pH 7. Fresh stock solutions were made of $ONOO^-$ (38–48 mM), SIN-1 (35 mM), as well as NO_2^-, NO_3^-, and NOC-7 (10–30 mM) when required, and the desired amount was added to the reaction. For experiments with decomposed $ONOO^-$ and NOC-7, stock solutions were allowed to decay overnight at room temperature, before incubation with PGHS-1. For samples analyzed by Western blotting, reactions of NO_x-treated PGHS-1 were treated for the designated times and then boiled for 5 min in SDS/mercaptoethanol buffer in preparation for immediate separation by SDS-PAGE. PGHS-1 (10 μM) was reacted with TNM (1 mM) for 1 h and used as a nitrated PGHS-1 marker in Western blot analysis (described below).

Modification of PGHS-1 with aspirin

Samples of soluble aspirin (0.5 mM) were prepared freshly from a 10 mM stock. To prepare 10 mM stock solutions, aspirin was first solubilized in 70% EtOH, followed by dilution with 0.9% NaCl. Aspirin was reacted with PGHS-1 at a 2.5:1.0 molar ratio for 10 min before coupled cyclooxygenase-peroxidase assays (described below).

Proteolysis of PGHS-1 and NO_x-treated PGHS-1 with LysC endoproteinase

PGHS-1 (5 mg; holo-, apo-, or $ONOO^-$-treated) was digested with 1 unit of LysC endoproteinase for 18 h at 37°C in 0.1 M NH_4HCO_3, pH 8.3. Detergents for PGHS-1 solubilization during purification were diluted to 0.07% βOG and 0.03% Tween-20. Proteolysis was stopped by the addition of SDS/mercaptoethanol, followed by rapid boiling for 5 min and separation by SDS-PAGE (10% acrylamide).

PGHS-1 activity assays

A peroxidase assay was used to measure PGHS-1 activity. This assay monitors the oxidation of TMPD by changes in absorbance at 611 nm after activation (33, 34). In some experiments, $ONOO^-$ was used as the activating species. In other experiments, the cyclooxygenase binding site substrate arachidonic acid was used as the activating species. We refer to assays using arachidonic acid as coupled cyclooxygenase-peroxidase assays. The standard reaction mixture in a spectrophotometer cuvette contained 1 ml of Tris buffer (0.1 M, pH 8.0), purified apoPGHS-1 enzyme (0.07 μM), hematin or hemin (0.1 μM), and TMPD (84 μM) from a 1 mg/ml stock solution. The reaction was initiated by the addition of arachidonic acid (0.1 mM). Maximal activity was achieved when 30% excess hemin was used to reconstitute apoPGHS-1 in the standard reaction mixture (data not shown). At 25°C, the ratio of TMPD oxidation to oxygen consumption by PGHS-1 in 60 s is 1 mol TMPD/1 mol O_2 (34). PGHS-1 activity is expressed as the rate of change in TMPD oxidation in 1 min.

Activity assays on $ONOO^-$-treated holoPGHS-1 were also measured at 611 nm as described above. Assays of $ONOO^-$-treated apoPGHS-1 activity were performed identically to holoPGHS-1 reactions except that hemin was added (0.1 μM) to the 1 ml cuvette before arachidonate. To determine whether $ONOO^-$ scavenges arachidonic acid in our reaction mixtures, we compared the mass spectrum of arachidonic acid (250 μM) with that of $ONOO^-$-treated arachidonic acid (250 μM each) and found them to be identical, indicating that arachidonic acid was not chemically altered to a significant extent by $ONOO^-$ (data not shown). Assays for the reaction of apoPGHS-1 and holoPGHS-1 with SIN-1, NO_3^-, NO_2^-, NOC-7, decomposed $ONOO^-$, and decomposed NOC-7 were also performed as described above for reactions with $ONOO^-$. For reactions in the presence of glutathione-peroxidase (GSH-Px) and GSH, concentrations in the reaction mixture and the assay chamber were kept at 25 U/ml and 0.25 mM, respectively. For reactions with the hydroxyl radical (•OH) scavenger EtOH, concentrations ranging from 10 to 1,000 mM were used. For reactions with the •OH scavengers L-NAME and potassium iodide (KI), concentrations ranging from 0.25 to 1.25 mM were used.

Detection of 3-nitrotyrosine in NO_x-treated, purified PGHS-1 by Western blotting

Two micrograms of protein per sample was treated with SDS/mercaptoethanol, separated on a 10% acrylamide gel, and transferred onto a nitrocellulose membrane (Bio-Rad). The membrane was immunoblotted with a mouse monoclonal 3-nitrotyrosine antibody according to the manufacturer's instructions (Upstate Biotechnology). The bands were revealed using enhanced chemiluminescence (ECL Plus) and visualized by scanning on a Storm 860 scanner. Blots were stripped by agitating at room temperature (10 min) in guanidinium chloride buffer (7 M) and reprobed with anti-mouse PGHS-1 antibody for 1 h.

Statistical analysis

All results were reproduced at least three times. Where appropriate, data are reported as averages ± SEM with significant differences determined by Student's *t*-test. $P < 0.05$ is statistically significant. Image J (version 1.34s) was used to quantify Western blot and SDS-PAGE band densities (National Institutes of Health).

RESULTS

Purification of ovine PGHS-1

Purification of detergent-extracted PGHS-1 on an anion-exchange DEAE-Sepharose column (Fig. 1A) is a critical step as it reduces the amount of PGHS-1 bound to natural lipids, allowing control of the detergent environment (35). Figure 1B shows an SDS-PAGE analysis of PGHS-1 (70 kDa) at three different stages of purification (see Methods). Homogenates from seminal vesicles (lane 2) and detergent-extracted microsomes (lane 3) contained considerable amounts of PGHS-1; however, many contaminating proteins were also present. Purification of PGHS-1 by the method used achieved purity levels (lane 4) comparable to those of commercially available ovine PGHS-1 (lane 1).

To investigate the effects of different detergents used in PGHS-1 purification on properties of the purified enzyme, we compared apoPGHS-1 solubilized in either

TABLE 1. Values of PGHS-1-bound heme and free heme in solution from reconstitutions

Detergent	Heme	$\Delta TMPD_{ox}$/min	Total Heme Concentration Needed for HoloPGHS-1 Concentration = 10 μM	Excess Heme Concentration[a]
βOG	Hemin	1.00 ± 0.05	14 μM	4 μM
βOG	Hematin	0.73 ± 0.05	35 μM	25 μM
Tween-20	Hemin	0.74 ± 0.02	35 μM	25 μM
Tween-20	Hematin	0.15 ± 0.02	61 μM	51 μM
CHAPS	Hemin	0.52 ± 0.02	35 μM	25 μM
CHAPS	Hematin	0.46 ± 0.02	46 μM	36 μM
Maltoside	Hemin	0.80 ± 0.02	23 μM	13 μM
Maltoside	Hematin	0.90 ± 0.01	46 μM	36 μM

βOG, *N*-octyl-β-D-glucopyranoside; PGHS-1, prostaglandin H_2 synthase-1; TMPD, *N,N,N′,N′*-tetramethylphenylenediamine.

[a] Excess heme concentration = total heme concentration − 10 μM.

Tween-20 or βOG after reconstitution with hemin to holoPGHS-1 (10 μM) containing heme at a 1:1 molar ratio. Heme-reconstituted PGHS-1 was then subjected to limited proteolysis with LysC endoproteinase and analyzed by SDS-PAGE (Fig. 1C). Undigested holoPGHS-1 in either Tween-20 (lane 1) or βOG (lane 3) have identical apparent masses at ~70 kDa. Residual PGHS-1 in βOG digest (lane 4; 47.85 ± 1.25%) was more abundant than PGHS-1 in Tween-20 digest (lane 2; 14.41 ± 0.81%), indicating that PGHS-1 in Tween-20 is more accessible to proteolysis and is possibly structurally compromised. Levels of detergent in samples were diluted before digestion to 0.07% βOG (from 0.4%) and 0.02% Tween-20 (from 0.1%) and are not expected to affect the action of LysC endoproteinase. In fact, previous studies show that the enzymatic activity of this endoproteinase is only affected by SDS, high NaCl concentrations (5 M), and prolonged exposure to temperatures of ≥70°C (36). This result suggests that the detergent composition influences the conformation of PGHS-1 and its accessibility to proteases.

Hemin-reconstituted PGHS-1 is stable and active in βOG

To determine the form of heme and detergent that best stabilizes active PGHS-1, purified apoPGHS-1 in Tween-20, CHAPS, $C_{10}M$, or βOG was reconstituted with hemin or hematin to yield a holoPGHS-1 concentration of 10 μM (**Table 1**). The concentration of holoPGHS-1 was calculated from the absorbance at 412 nm using a molar extinction coefficient of 142,000 $M^{-1}cm^{-1}$ (described in Materials and Methods). Table 1 shows that with all four detergents, a larger amount of heme is incorporated into apoPGHS-1 when it is supplied as hemin. This is evident from the lower concentrations of hemin required to reconstitute identical apoPGHS-1 samples. Conversely, the concentration of free hematin in solution for each trial exceeds that of free hemin. Among the four detergents used for PGHS-1 solubilization, PGHS-1 in βOG required the least amount of heme for reconstitution, as opposed to PGHS-1 in Tween-20, which needed the highest concentration. Furthermore, holoPGHS-1 solubilized in βOG and, in particular, if reconstituted with hemin was most active, as opposed to the least active holoPGHS-1 that is reconstituted with hematin and solubilized in Tween-20 (Table 1). For optimal activity, all subsequent experiments described herein used PGHS-1 solubilized in βOG and holoPGHS-1 reconstituted with hemin.

The effect of $ONOO^-$ on PGHS-1 catalysis is independent of the cyclooxygenase binding site

We have shown previously that micromolar concentrations of $ONOO^-$ enhanced PGHS-1 activity in purified protein and in smooth muscle cells treated with arachidonic acid. Accordingly, we postulated that $ONOO^-$ acts as a peroxide initiator at the iron center of the peroxidase site (15). To test whether $ONOO^-$ initiation of peroxidase activity involves the cyclooxygenase site, we inhibited the cyclooxygenase site with aspirin (25 μM, 10 min) and initiated peroxidase activity with arachidonic acid (**Fig. 2A**) as well as with $ONOO^-$ (Fig. 2B). Figure 2A shows that when we measured peroxidase activity in the presence of arachidonic acid (25 μM), activity was sig-

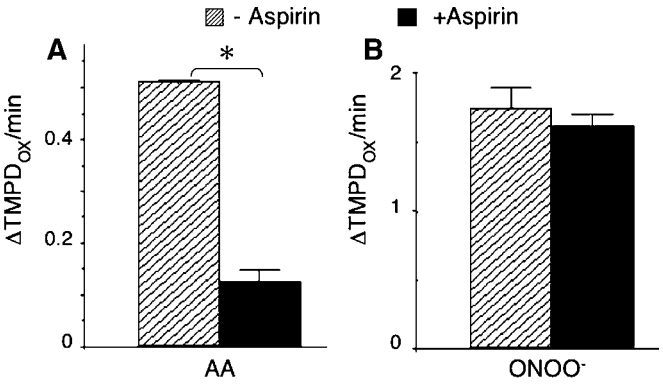

Fig. 2. Effect of peroxynitrite ($ONOO^-$) on PGHS-1 catalysis is independent of the cyclooxygenase binding site. A: Cyclooxygenase-coupled peroxidase activity measured in the presence of arachidonic acid (AA; 100 μM) was significantly reduced for aspirin-treated holoPGHS-1 (black bars) compared with holoPGHS-1 (diagonal bars). B: $ONOO^-$ (250 μM) equally activated the peroxidase function of holoPGHS-1 (diagonal bars) and aspirin-treated holoPGHS-1 (black bars) without arachidonic acid. The results are expressed as the change in absorbance at 611 nm in 60 s as a result of *N,N,N′,N′*-tetramethylphenylenediamine (TMPD) oxidation. The concentrations of holoPGHS-1 and aspirin were 10 and 25 μM, respectively. These concentrations were diluted during activity assays (see Materials and Methods). Data shown are averages ± SEM. * $P < 0.001$.

nificantly inhibited by aspirin. In contrast, Fig. 2B shows that $ONOO^-$ (250 μM) activated peroxidase function (in the absence of arachidonic acid) and aspirin had no impact on the level of activation. Results from Fig. 2 demonstrate that the cyclooxygenase site is vital for generating the necessary initiating peroxide from arachidonic acid, whereas $ONOO^-$ acts directly as the activating peroxide at the heme center. Thus, in the case of arachidonic acid, we are measuring cyclooxygenase-coupled peroxidase activity. In contrast, $ONOO^-$ activates solely at the peroxidase site.

$ONOO^-$ modulation of PGHS-1 reactivity is heme-dependent

Although the experiments described above demonstrate that $ONOO^-$ provides the peroxide tone to activate peroxidase function, it is also known to modify proteins, causing typical loss of function. In the presence of arachidonic acid, initiation of peroxidase activity by $ONOO^-$ leads to enhanced eicosanoid production (15, 17, 25). We hypothesized that in the absence of arachidonic acid, peroxidase activation by $ONOO^-$ will render the enzyme incapable of any subsequent arachidonic acid metabolism. Therefore, we examined the effect of preincubating holoPGHS-1 and apoPGHS-1 with $ONOO^-$ for varying time periods in HEPES buffer (pH 7) on cyclooxygenase-coupled peroxidase activity using arachidonic acid as substrate (see above). Note that it was necessary to add hemin to the apoPGHS-1 sample at the time of the activity assay. In the absence of $ONOO^-$, activity levels of apoPGHS-1 and holoPGHS-1 remained unchanged for up to 3 h at room temperature. Preincubation of holoPGHS-1 (containing heme) with $ONOO^-$ (250 μM) for 2 min almost abolished arachidonic acid metabolism (**Fig. 3A**, black bars). However, apoPGHS-1 (without heme) pretreated for 2 min with $ONOO^-$ retained its ability to metabolize arachidonic acid once reconstituted with heme, and activity was not different from the control level (Fig. 3A, gray bars). Concentrations of $ONOO^-$ >250 μM resulted in very rapid deactivation of holoPGHS-1, whereas concentrations <150 μM had unreliable effects on activity (data not shown). Reconstitution of PGHS-1 with excess hemin results in some free hemin, which could potentially react with $ONOO^-$ and contribute to loss of activity in PGHS-1. To test the effect of free hemin on PGHS-1 activity in the presence of $ONOO^-$ (250 μM), we performed a stoichiometric titration of apoPGHS-1 with hemin, followed by exposure to $ONOO^-$ and activity measurements. The reconstituted hemin:PGHS-1 complexes (1.3:1, 1:1, and 0.75:1) were equally deactivated after $ONOO^-$ treatment for 2 min, indicating that potential reactions between excess hemin and $ONOO^-$ do not contribute significantly to holoPGHS-1 deactivation under our experimental conditions (data not shown). We also added a hemin/$ONOO^-$ mixture to holoPGHS-1 and determined the effect on activity. The hemin/$ONOO^-$ mixture also had no effect on holoPGHS-1 activity.

Similar to $ONOO^-$, preincubation of holoPGHS-1 with the $ONOO^-$ donor molecule SIN-1 (2 mM) inhibited arachidonic acid metabolism. The loss in activity was as extensive as that observed with $ONOO^-$ (Fig. 3B) but occurred over a longer time period (3 h). This reflects the slow decomposition of SIN-1 to $ONOO^-$ (37). Concentrations of SIN-1 <1 mM did not impair PGHS-1 activity, whereas higher concentrations resulted in loss of activity in a dose-dependent manner (data not shown). Preincubation of apoPGHS-1 with SIN-1 (2 mM) had no effect on arachidonic acid metabolism (data not shown). Preincubation with NOC-7 (250 μM–2 mM), NO_2^- (250–500 μM), NO_3^- (250–500 μM), and decomposed $ONOO^-$ (250–500 μM) had no effect on PGHS-1 activity under our experimental conditions (data not shown). These results

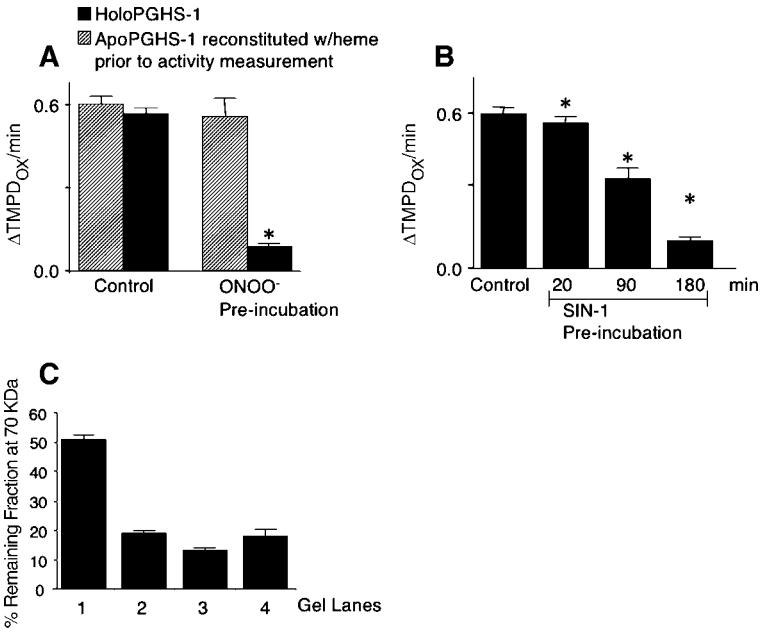

Fig. 3. $ONOO^-$ modulation of PGHS-1 reactivity is heme-dependent. A: HoloPGHS-1 (black bars) and apoPGHS-1 (gray bars) were preincubated with $ONOO^-$ (250 μM) for 2 min, and enzyme activity was measured after the addition of arachidonic acid (100 μM) in 20 mM HEPES buffer, pH 7.0. For apoPGHS-1, hemin was added at the time of activity measurement. Control apoPGHS-1 and holoPGHS-1 samples have no added $ONOO^-$. Results are expressed as the change in absorbance at 611 nm in 60 s as a result of TMPD oxidation. B: Enzyme activity was measured in a similar manner to A after preincubation of holoPGHS-1 with 3-morpholinosydnonimine hydrochloride (SIN-1; 2 mM) at different time points. C: Percentage remaining digested fractions at 70 kDa from SDS-PAGE analysis of LysC endoproteinase digests (0.6 units, 18 h) of holoPGHS-1 (lane 1), apoPGHS-1 (lane 2), $ONOO^-$-treated holoPGHS-1 (lane 3), and $ONOO^-$-treated apoPGHS-1 (lane 4). The concentrations of PGHS-1 and $ONOO^-$ in the reaction mixtures were 10 and 250 μM, respectively, and treatments with $ONOO^-$ were for 1 h. These concentrations were diluted during activity assays (see Materials and Methods). Data shown are averages ± SEM. * $P < 0.05$ relative to control.

indicate that in the presence of heme, $ONOO^-$ and SIN-1 lead to a modification in PGHS-1 that abolishes subsequent arachidonic acid metabolism. In contrast, preincubation of apoPGHS-1 with $ONOO^-$ and SIN-1 did not affect the enzyme's ability to reconstitute heme and exhibit full activity.

To probe the effect of $ONOO^-$ on the structure of PGHS-1, $ONOO^-$ reacted with both holoPGHS-1 and apoPGHS-1 was examined for susceptibility to proteolytic cleavage. Changes in secondary structure can render the protein more accessible to proteases. Notably, $ONOO^-$ treatment was found to alter the protease digestion patterns of PGHS-1 (Fig. 3C). Equal concentrations of holoPGHS-1, apoPGHS-1, $ONOO^-$-treated holoPGHS-1, and $ONOO^-$-treated apoPGHS-1 were digested with LysC endoproteinase and analyzed by SDS-PAGE, as described in Materials and Methods. As expected, the percentage of undigested fraction of holoPGHS-1 at 70 kDa (lane 1) was greater than that of apoPGHS-1 (lane 2), suggesting that holoPGHS-1 is less solvent-exposed and more resistant to proteolysis than apoPGHS-1. $ONOO^-$-treated holoPGHS-1 (lane 3) also digested much more extensively than untreated holoPGHS-1 (lane 1) and to a similar extent to apoPGHS-1, with and without $ONOO^-$ (lanes 2, 4). These results suggest that the secondary structure of holoPGHS-1 is compromised by $ONOO^-$ treatment.

$ONOO^-$ and SIN-1 induce Tyr 385 nitration in holoPGHS-1 but not in apoPGHS-1

To map variations in nitration sites between apoPGHS-1 and holoPGHS-1 after their reactions with either $ONOO^-$ (1 mM) or SIN-1 (2 mM), proteins were subjected to trypsinolysis and peptide products were analyzed by nLC-MS/MS, as described in Materials and Methods. **Figure 4A, B** shows extracted ion chromatograms at *m/z* 645.5 for $ONOO^-$-treated holoPGHS-1, $ONOO^-$-treated apoPGHS-1, SIN-1-treated holoPGHS-1, and SIN-1-treated apoPGHS-1. The peptide ion at ~38 min represents the quadruple-charged peptide ion IAMEFNQLYHWHPLMPDSFR (iso-

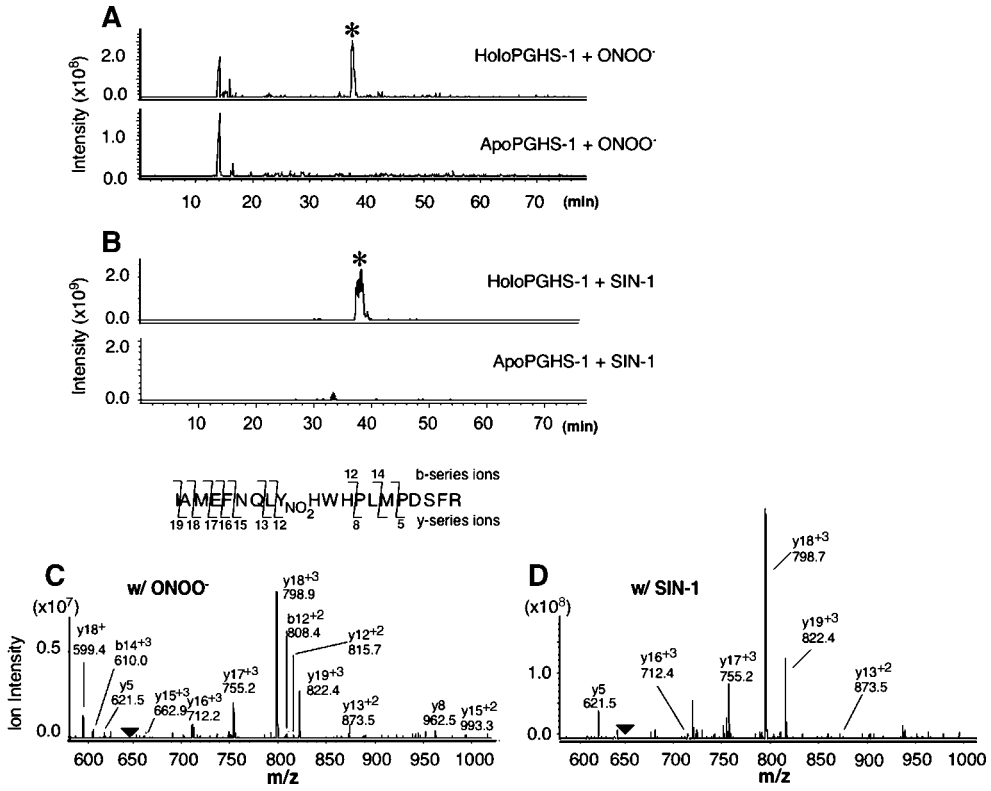

Fig. 4. $ONOO^-$ and SIN-1 induce tyrosine 385 (Tyr 385) nitration in holoPGHS-1 but not apoPGHS-1. HoloPGHS-1 (8 μM) and apoPGHS-1 (8 μM) were incubated with $ONOO^-$ (1 mM) or SIN-1 (2 mM) for 1 h and subjected to acetone precipitation, resuspension in ammonium bicarbonate, reduction, and alkylation (as described in Materials and Methods). The samples were digested with 0.3% trypsin overnight and analyzed by nanoflow liquid chromatography-tandem mass spectrometry (nLC-MS/MS). A, B: Extracted ion chromatograms for the peptide fragment (*m/z* 645.5) representing the quadruple-charged peptide ion IAMEFNQLYHWHPLMPDSFR that is nitrated at the Tyr residue. The extracted ion chromatograms monitor LC elution of this peptide ion with time for $ONOO^-$-treated holoPGHS-1, $ONOO^-$-treated apoPGHS-1, SIN-1-treated holoPGHS-1, and SIN-1-treated apoPGHS-1. The asterisks at ~38 min in the elution profiles in the top panels of A and B denote a peptide of *m/z* 645.5 that is missing in $ONOO^-$-treated apoPGHS-1 and SIN-1-treated apoPGHS-1 (bottom panels). C, D: MS/MS analysis of the peptide ion eluting at ~38 min from $ONOO^-$-treated holoPGHS-1 (C) and SIN-1-treated holoPGHS-1 (D) confirms the identity of this peptide sequence as IAMEFNQLYHWHPLMPDSFR containing nitrated Tyr 385. Black arrowheads denote the parent ion at *m/z* 645.5 from which the depicted daughter ions arise.

leucine 377–arginine 396), which is nitrated at Tyr 385. The nitrated peptide ion was observed in the $ONOO^-$-treated holoPGHS-1 and SIN-1-treated holoPGHS-1 samples (~38 min, indicated by asterisks) but was absent from the $ONOO^-$- and SIN-1-treated apoPGHS-1 samples. Fragmentation of this peptide ion (*m/z* 645.5) by MS/MS from $ONOO^-$-treated holoPGHS-1 and SIN-1-treated holoPGHS-1 confirmed its identity as nitrated Tyr 385 peptide (Fig. 4C, D). The untreated apoPGHS-1 and holoPGHS-1 samples did not show evidence of the nitrated peptide ion, as expected (data not shown). The corresponding unmodified peptide ion (isoleucine 377–arginine 396) with *m/z* 634.3 was present in all samples (data not shown).

Figure 5 shows overlays of extracted ion chromatograms that compare peak areas for the Tyr 385 nitrated peptide ion (*m/z* 645.5) and its corresponding unmodified peptide ion (*m/z* 634.3) from the reactions of SIN-1 with apoPGHS-1 (Fig. 5A) and holoPGHS-1 (Fig. 5B). Figure 5B shows that SIN-1-treated holoPGHS-1 results in almost equal intensity peaks at ~38 min (black trace, nitrated peptide ion) and at ~32 min (red trace, unmodified peptide ion), suggesting that ~50% Tyr 385 nitration in holoPGHS-1 is achieved by SIN-1. In contrast, SIN-1-treated apoPGHS-1 (Fig. 5A) produces a peak only at ~32 min (green trace), indicating that SIN-1 did not result in Tyr 385 nitration in apoPGHS-1. Similarly, we estimate the percentage of Tyr 385 nitration in $ONOO^-$-treated holoPGHS-1 to be ~50% (data not shown). These results confirm that the heme is required for Tyr 385 nitration in PGHS-1.

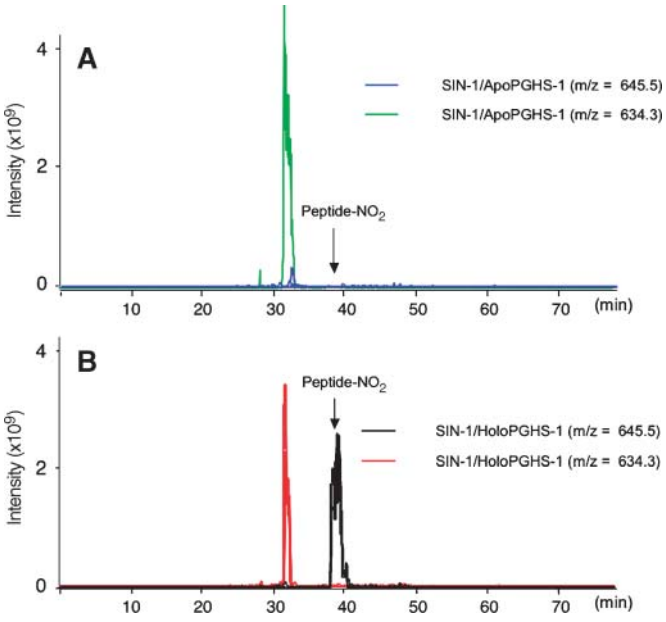

Fig. 5. Extracted ion chromatograms of nitrated and unmodified peptide ions for SIN-1-treated holoPGHS-1 and apoPGHS-1. Extracted ion chromatogram overlays for SIN-1-treated apoPGHS-1 (A) and SIN-1-treated holoPGHS-1 (B) (2 mM SIN-1) compare peak areas of the nitrated peptide ion (IAMEFNQLYHWHPLMPDSFR) at Tyr 385 (*m/z* 645.5, ~38 min) and its corresponding nonnitrated peptide ion (*m/z* 634.3, ~32 min).

$ONOO^-$ changes the heme Soret band intensity of holoPGHS-1

The effect of preincubating holoPGHS-1 with $ONOO^-$ on the extensive activity loss was further investigated by monitoring the heme Soret band at 412 nm (**Fig. 6A**). ApoPGHS-1 (10 μM) gives a relatively flat spectrum consistent with heme depletion (spectrum a), which, when reconstituted with hemin (~1:1 heme:protein molar ratio), gives rise to the heme-replete spectrum b in Fig. 6A. The corresponding enzymatic activity profile for holoPGHS-1 is shown in Fig. 6B (profile b). Although deactivation of holoPGHS-1 by $ONOO^-$ occurs within 2 min, for ease and consistency of experimentation, we monitored reactions for 1 h. The UV-Vis spectrum and corresponding activity profile (measured by adding 100 μM arachidonic acid) of holoPGHS-1 did not change over the course of 1 h in the absence of $ONOO^-$. When holoPGHS-1 was incubated with $ONOO^-$, the Soret maximum at 412 nm decreased by 50% within 2 min and remained unchanged during the course of 1 h (Fig. 6A, spectrum c); notably, this was accompanied by a 90% loss in PGHS-1 activity (Fig. 6B, profile c). The addition of fresh hemin (5 μM) to $ONOO^-$-treated holoPGHS-1 appeared to restore absorbance at 412 nm to control levels (data not shown), but interestingly, the protein exhibited only 34% of its original ability to metabolize arachidonic acid (Fig. 6B, profile d). The disproportionality between remaining Soret absorbance and activity loss suggests that *i*) a modification that is heme-related (e.g., heme loss, modification of heme, formation of heme-protein adducts) and/or *ii*) $ONOO^-$-mediated modifications to the polypeptide backbone (e.g., Tyr 385 nitration) occurred. To determine the fate of heme after $ONOO^-$ reaction with holoPGHS-1, we analyzed the nature of free heme obtained from holoPGHS-1 and $ONOO^-$-treated holoPGHS-1 by MALDI-TOF mass spectrometry. This method allows us to detect free heme that may be released as a result of $ONOO^-$ (or as a result of the MALDI-TOF process). No changes in free heme spectra were observed between untreated and $ONOO^-$-treated holoPGHS-1 samples (data not shown), suggesting that $ONOO^-$ did not modify heme from holoPGHS-1.

On reacting holoPGHS-1 with NOC-7 (250 and 750 μM), no changes in enzymatic activity or heme Soret spectra occurred (compared with nonreacted holoPGHS-1) during a 1 h incubation period (data not shown). These data indicate that $ONOO^-$, but not NO from NOC-7, suppresses holoPGHS-1 metabolism of arachidonic acid under the test conditions.

To determine whether the $ONOO^-$-induced PGHS-1 loss of function was attributable to its inherent peroxide nature, the heme Soret band of PGHS-1 was monitored in the presence of $ONOO^-$ and a hydroperoxide scavenging system comprising GSH-Px (24 U/200 μl) and GSH (0.25 mM) (Fig. 6C). Although little or no decrease in absorbance at 412 nm occurred after 1 h of $ONOO^-$ exposure (Fig. 6C, spectrum c), the enzyme lost 50% of its activity (Fig. 6D, profile c). Addition of fresh hemin (5 μM) to $ONOO^-$-treated holoPGHS-1 in the presence of GSH-Px/GSH restored 80% of enzymatic activity (Fig. 6D,

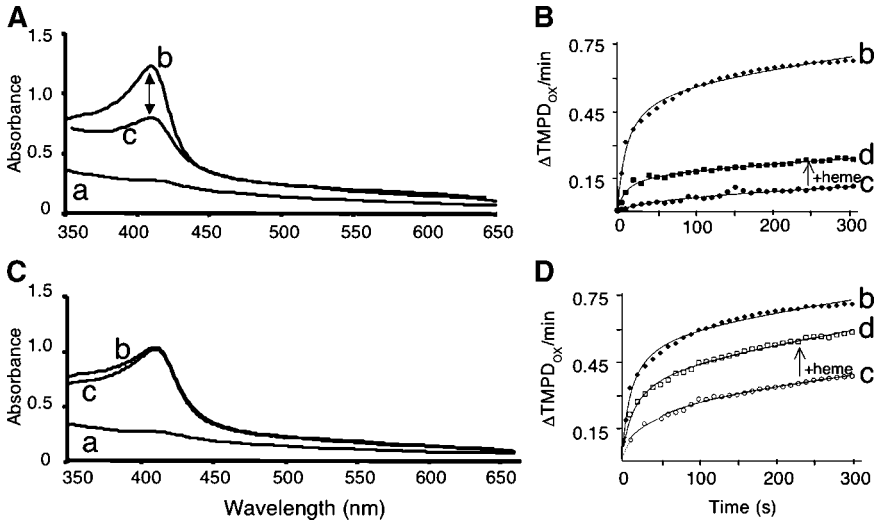

Fig. 6. ONOO$^-$ decreases heme Soret absorption in holoPGHS-1. A: Absorbance spectra were acquired after incubation of holoPGHS-1 with ONOO$^-$ for 1 h. B: Enzyme activity profiles acquired by adding arachidonic acid (100 μM) after preincubation of holoPGHS-1 with ONOO$^-$ for 1 h. C: Absorbance spectra were acquired similarly to A but in the presence of GSH-Px (24 U/200 μl)/GSH (0.25 mM). D: Enzyme activity profiles acquired similarly to B but in the presence of GSH-Px (24 U/200 μl)/GSH (0.25 mM). The recorded spectra and profiles are as follows: a, apoPGHS-1; b, holoPGHS-1; c, ONOO$^-$-treated holoPGHS-1; and d, freshly added hemin (5 μM) to the sample from c. The concentrations of PGHS-1 and ONOO$^-$ were 10 and 250 μM, respectively.

profile d). Note that the control spectra of holoPGHS-1 in Fig. 6A, C were obtained by reconstituting with identical concentrations of heme. In the presence of GSH-Px/GSH, the Soret maximum for the holoPGHS-1 control was slightly reduced from the control in the absence of GSH-Px/GSH, indicating that GSH-Px/GSH interferes with heme reconstitution of PGHS-1. In fact, addition of fresh hemin actually resulted in the Soret band intensity increasing to the levels observed in Fig. 6A (data not shown), which may account for the increased activity. Additionally, a dose-response study of ONOO$^-$ (50–250 μM) with holoPGHS-1 showed that increasing concentrations of ONOO$^-$ resulted in a decrease in the Soret band at 410 nm and reached a plateau at ~50–60%. However, loss of enzyme activity increased progressively with ONOO$^-$ concentrations (data not shown). The GSH-Px/GSH mixture may effectively decrease ONOO$^-$ concentrations, with the result that activity was less impaired (15) and no loss of heme Soret absorption. In summary, these data show that the antioxidant system provided partial protection against ONOO$^-$-induced processes that contribute to PGHS-1 activity loss.

·OH scavengers do not protect PGHS-1 from inactivation by ONOO$^-$

To investigate whether ·OH generated by ONOO$^-$ homolysis contributes to the loss of holoPGHS-1 function, we used EtOH as a scavenger of ·OH (38). In additional studies, we assessed whether inactivation of PGHS-1 by ONOO$^-$ is attenuated by KI, a scavenger of ·OH, H_2O_2, and triplet oxygen (39), as well as by L-NAME. Although L-NAME is a nitric oxide synthase inhibitor, it can also scavenge ·OH directly and more quickly than the established ·OH scavenger mannitol and without interfering with ONOO$^-$ oxidation chemistry (40). EtOH (100 mM) (**Fig. 7**, dark gray bars) and L-NAME (1.25 mM) (Fig. 7, light gray bars) showed no protection from the deleterious effects of ONOO$^-$, whereas KI (1.25 mM) (Fig. 7, white bars) showed a significant improvement compared with EtOH and L-NAME. Activity assays were also performed using a range of scavenger concentrations (described in

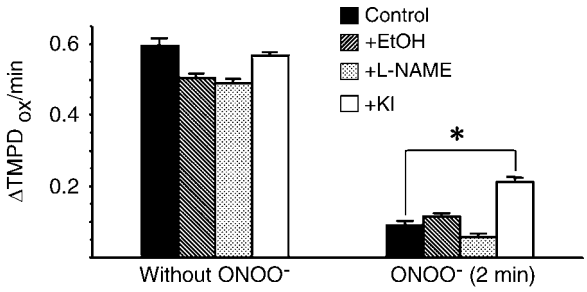

Fig. 7. Hydroxyl radical scavengers do not protect PGHS-1 from deactivation by ONOO$^-$. HoloPGHS-1 was preincubated with ONOO$^-$ for 2 min in the presence and absence of ethanol (EtOH), N^G-nitro-L-arginine methyl ester (L-NAME), or potassium iodide (KI), and enzyme activity was measured after the addition of arachidonic acid (100 μM). The black bars represent enzyme activity in the absence of EtOH, L-NAME, or KI. The dark gray bars represent enzyme activity in the presence of EtOH (100 mM). The light gray bars represent enzyme activity in the presence of L-NAME (1.25 mM). The white bars represent enzyme activity in the presence of KI (1.25 mM). The concentrations of PGHS-1 and ONOO$^-$ in the reaction mixtures were 10 and 250 μM, respectively. These concentrations were diluted during activity assays (see Materials and Methods). Results are expressed as the change in absorbance at 611 nm in 60 s as a result of TMPD oxidation. Data shown are averages ± SEM. * $P < 0.005$.

Materials and Methods), with results similar to those observed in Fig. 7. These results suggest that loss of PGHS-1 activity is mediated by a direct action of $ONOO^-$ and does not involve the secondary oxidant $^{\bullet}OH$.

Tyrosine nitration of PGHS-1 by $ONOO^-$ and SIN-1 is enhanced by heme

As demonstrated above, PGHS-1 inactivation and Tyr 385 nitration by $ONOO^-$ and SIN-1 are directed by heme. In addition, the disproportionality between the extensive loss of activity in $ONOO^-$-treated PGHS-1 and the remaining 50% heme Soret absorbance led us to investigate levels of PGHS-1 nitration by $ONOO^-$ and SIN-1 in the presence and absence of heme. By Western blot analysis with a anti-nitrotyrosine antibody, we examined the extent of PGHS-1 Tyr nitration by $ONOO^-$ as a function of time in the presence and absence of hemin and arachidonic acid (**Fig. 8A**, **B**). Under our experimental conditions, NO_2^-, NO_3^-, NOC-7, and decomposed $ONOO^-$ did not nitrate PGHS-1 (data not shown). Tyr nitration of both holoPGHS-1 (Fig. 8A, top blot) and apoPGHS-1 (Fig. 8B, top blot) was complete within 2 min of $ONOO^-$ exposure in the presence and absence of arachidonic acid (100 μM). However, nitration was more extensive in holoPGHS-1 compared with apoPGHS-1. Treatment of holoPGHS-1 with $ONOO^-$ resulted in the appearance of bands at apparent molecular masses as high as ~250 kDa, indicating the presence of nitrated PGHS-1 multimers (Fig. 8A, top blot). These nitrated multimers were absent from $ONOO^-$-treated apoPGHS-1 (Fig. 8B, top blot). These results suggest that the heme group promotes $ONOO^-$-elicited multimer formation and amplifies nitration levels. Arachidonic acid appeared to reduce nitration levels in both $ONOO^-$-treated holoPGHS-1 and apoPGHS-1 (Fig. 8A, B) but increased levels of nitrated high molecular mass species in holoPGHS-1 (Fig. 8A). Loss of nitration in the presence of arachidonic acid is likely attributable to its binding in the cyclooxygenase channel, blocking access of nitrating species to Tyr 385. Notably, mass spectrometric analysis (described in Materials and Methods) confirmed that arachidonic acid did not chemically react with $ONOO^-$ to a detectable extent under the reaction conditions used (data not shown).

The extents of Tyr nitration by SIN-1 of holoPGHS-1 and apoPGHS-1 were also compared by Western blot analysis (Fig. 8C). Quantitation of nitrated PGHS-1 band intensities relative to equal PGHS-1 protein loading show that SIN-1 (5 mM) nitrated holoPGHS-1 (white bars) more extensively than apoPGHS-1 (black bars) in a time-dependent manner. Similar results were observed with 2 mM SIN-1 (data not shown). Results for PGHS-1 nitration by SIN-1 are consistent with the results obtained with $ONOO^-$ and indicate that Tyr nitration in the absence of heme does occur (even at low steady-state levels of SIN-1-derived $ONOO^-$), but with no effect on enzyme activity unless heme is present. In summary, these results show that in the presence of heme, there is enhancement of overall PGHS-1 nitration and aggregation and specific nitration of Tyr 385, which may play a pivotal role in PGHS-1 inactivation.

DISCUSSION

In these studies, we developed conditions to prepare large quantities of purified PGHS-1 using regular-flow liquid chromatography (Fig. 1). It was critical to determine PGHS-1 detergent solubilization and heme reconstitution conditions that limited enzyme inactivation or denaturation and allowed for reproducible activity. We

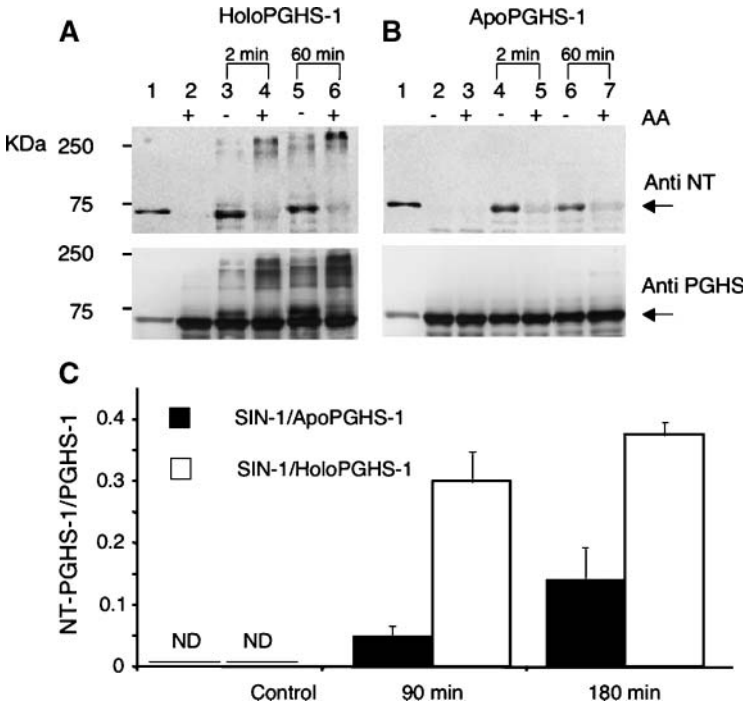

Fig. 8. Tyrosine nitration of PGHS-1 by $ONOO^-$ is enhanced by heme. Western blots for the reaction of purified holoPGHS-1 (10 μM) (A) and apoPGHS-1 (10 μM) (B) with $ONOO^-$ (250 μM) in the presence (+) and absence (−) of arachidonic acid (AA; 100 μM) as a function of time. Blots were probed with monoclonal anti-nitrotyrosine (Anti NT) antibody (top) and then stripped and reprobed with monoclonal PGHS-1 antibody (bottom). Lane 1 in A and B represents PGHS-1 that has been nitrated by tetranitromethane and serves as a nitrated PGHS-1 control. Lane 2 (A, B) and lane 3 (B) represent PGHS-1 controls in the absence of $ONOO^-$. C: Reaction of purified apoPGHS-1 (10 μM; black bars) and holoPGHS-1 (10 μM; white bars) with SIN-1 (5 mM) as a function of time. Reactions were probed by Western blotting with monoclonal anti-nitrotyrosine antibody and then stripped and reprobed with monoclonal PGHS-1 antibody. Relative nitration was obtained by quantifying band density ratios between nitrated PGHS-1 and total PGHS-1 for each reaction. Control has no added SIN-1. HEPES (20 mM) was used in all samples. ND, not detected. Data shown are averages ± SEM.

found that βOG was most stabilizing to enzyme activity, whereas the commonly used Tween-20 was least stabilizing. In addition, we found that the detergent influences the structure of PGHS-1. In this regard, PGHS-1 proteolysis was limited when solubilized in βOG compared with Tween-20 (Fig. 1C), suggesting that PGHS-1 possesses a more ordered structure in βOG. Reconstitution profiles with hemin and the more commonly used hematin (Table 1) indicated that with all four solubilization detergents, hemin incorporated more readily into apoPGHS-1, especially when βOG was the detergent of choice. It is possible that the propensity of hematin to form μ-oxo dimers (41) interferes with PGHS-1 reconstitution and may explain the larger concentrations of hematin required, compared with hemin. In summary, solubilization of PGHS-1 in βOG and reconstitution with hemin provided the most optimal conditions for solution studies with purified PGHS-1.

This study implemented peroxidase assays to investigate the peroxidase activity of PGHS-1. It is known that binding of arachidonic acid to the cyclooxygenase binding site generates the cyclic endoperoxide prostaglandin G_2, which is reduced to prostaglandin H_2 at the peroxidase site. Therefore, when using arachidonic acid, the peroxidase assay actually measures a coupled cyclooxygenase-peroxidase function. Our studies using aspirin show that $ONOO^-$ acts solely at the peroxidase site of PGHS-1 and independently of the cyclooxygenase site (Fig. 2). It is important to note here that although $ONOO^-$ concentrations used in this study (250 μM) are seemingly high, the active species is extremely short-lived. The half-life of $ONOO^-$ is ~1 s under physiological conditions, and 250 μM $ONOO^-$ decays in seconds to nanomolar concentrations (42). For instance, a bolus addition of 250 μM $ONOO^-$ decays to ~0.4 μM in 10 s and to ~0.7 nM in 20 s.

Using the cyclooxygenase-coupled peroxidase assay, we investigated whether PGHS-1 can be activated following NO_x exposure. For these experiments, we measured enzymatic activity at different times after incubation of apoPGHS-1 and holoPGHS-1 with NO_x (Fig. 3A, B). HoloPGHS-1 exposed to $ONOO^-$ for 2 min could not metabolize arachidonic acid, whereas apoPGHS-1 activity was not decreased under these conditions. Incubation of holoPGHS-1 with SIN-1, which provides a system that slowly and continuously delivers low levels of both superoxide (7.02 μM/min) and NO (3.68 μM/min) (37) that combine at rates near the diffusion-controlled limit to form $ONOO^-$ (43), also resulted in an extensive activity loss, but at a slower rate than directly added $ONOO^-$. Deactivation of PGHS-1 by $ONOO^-$ can potentially occur through oxidative damage to the peroxidase site (e.g., heme loss, modification of heme, formation of heme-protein adducts) and/or modification of amino acids in the polypeptide backbone that are essential to structure and function (24, 25, 27, 32). PGHS-1 metabolism of arachidonic acid was not affected by preincubation with NO_2^-, NO_3^-, NOC-7, and decomposed $ONOO^-$, suggesting that $ONOO^-$ is the relevant inhibitory NO_x. Proteolysis combined with SDS-PAGE analysis (Fig. 3C) was used to probe for secondary structure changes in PGHS-1 in response to $ONOO^-$ treatment. $ONOO^-$-treated holoPGHS-1 digested more extensively than $ONOO^-$-treated apoPGHS-1, indicating that the structure of holoPGHS-1 is compromised (i.e., becomes less rigid) after reaction with $ONOO^-$. nLC-MS/MS analysis of $ONOO^-$-treated and SIN-1-treated holoPGHS-1 (Fig. 4) revealed Tyr 385 nitration, which was undetectable in $ONOO^-$-treated and SIN-1-treated apoPGHS-1. The percentage of Tyr 385 nitration by $ONOO^-$ and SIN-1 (Fig. 5) may exceed 50% under our reaction conditions. These results indicate that the heme is required for Tyr 385 nitration in PGHS-1 by $ONOO^-$ and SIN-1.

UV-Vis spectral analyses were conducted in an attempt to correlate changes in enzyme activity with changes in heme Soret absorption (Fig. 6A, B). We found that preincubation of holoPGHS-1 with $ONOO^-$ destroyed 90% of subsequent enzyme function but retained ~50% of the Soret absorbance, whereas NOC-7 and decomposed $ONOO^-$ had no effect on either. Furthermore, fresh heme additions to $ONOO^-$-treated PGHS-1 did not reinstate full activity. It is possible that loss of function by $ONOO^-$ can occur through heme loss and/or alterations of the heme, including heme-protein adducts or modified heme that interferes with activity but continues to absorb in the Soret region (50% Soret absorbance/90% loss in activity). MALDI-TOF analysis of free heme that could be released as a result of $ONOO^-$ addition (or as a result of the MALDI-TOF process) did not reveal heme modification attributable to the $ONOO^-$ reaction. An altered form of PGHS-1 that is inactive could involve heme-PGHS-1 adduct formation. A covalently modified porphyrin-PGHS-1 complex has been detected for deactivated PGHS-1 in the presence of cyclooxygenase inhibitors (32). Another inactive form may involve thiol oxidation of cysteine residues (44). PGHS-1 contains three surface cysteine residues (cysteines 313, 512, and 540), which are potential targets for oxidative modification. Mutagenesis studies have shown that although these cysteine residues are not essential for cyclooxygenase activity, they do contribute to the structural integrity of PGHS-1 (45). Although *S*-nitroso-*N*-acetylpenicillamine, an agent that *S*-nitrosates cysteine residues (46), had no effect on PGHS-1 activity (15, 17), it was recently reported that *S*-nitrosation enhances the activation of PGHS-2 (18). $ONOO^-$ has been reported to generate *S*-nitroglutathione from GSH (47) and is involved in the formation of sulfenic (-SO), sulfinic ($-SO_2$), and sulfonic ($-SO_3$) moieties (44). Thus, the involvement of cysteine oxidation in PGHS-1 function cannot be discounted and will be the focus of separate studies. Chemical modification of PGHS-1 by $ONOO^-$ also involves the nitration of Tyr residues (24) and was the focus of this study. Our findings reveal that the heme group catalyzes the modification of Tyr 385 that is essential to PGHS-1 function.

Studies were performed to determine the nature of the PGHS-1-inactivating species that may derive from $ONOO^-$, as well as the conditions under which we can protect enzymatic function from this species. GSH and GSH-Px destroy hydroperoxides (48) and are efficient scavengers of $ONOO^-$ (44, 49). Our results (Fig. 6C, D)

indicate that GSH-Px/GSH prevented changes to the Soret maximum at 412 nm but only partially protected against $ONOO^-$-induced processes that contribute to the loss of PGHS-1 activity. PGHS-1 inactivation by $ONOO^-$ was also partially prevented by KI (Fig. 7). Although KI scavenges $^{\bullet}OH$, it is nonspecific and also scavenges H_2O_2 (39). Thus, some of the protective effect offered by KI is of a similar nature to that offered by GSH-Px/GSH in scavenging $ONOO^-$. The $^{\bullet}OH$ scavenger EtOH as well as L-NAME, which is a specific scavenger of $^{\bullet}OH$ but not $ONOO^-$ or $ONOO^-$-derived nitrating species, had no effect on PGHS-1 deactivation by $ONOO^-$. L-NAME is reported to be more effective than mannitol at scavenging $^{\bullet}OH$ (40). Therefore, deactivation of PGHS-1 appears not to involve the secondary oxidizing intermediate $^{\bullet}OH$ but may occur by direct reaction with $ONOO^-$.

Nitration of aromatic Tyr residues by $ONOO^-$ was demonstrated previously in PGHS (24, 25). However, the role of the PGHS-1 heme group and arachidonic acid substrate in Tyr modification had not been examined. One important observation made in our study is that nitration of apoPGHS-1 does not interfere with its ability to reconstitute heme and metabolize arachidonic acid. However, mass spectrometric and Western blotting results depicted in Figs. 4, 5, and 8 demonstrate that heme catalyzes the nitration of Tyr 385 in PGHS-1 by $ONOO^-$ and SIN-1; importantly, this residue is critical to enzyme activity (11, 28). A similar phenomenon has been described for ferric hemoglobin and cytochrome P450 in the presence of $ONOO^-$ (50, 51). We conclude that in the presence of $ONOO^-$, the heme group of PGHS-1 catalyzes its own demise by inducing the nitration of a Tyr residue that is critical for activity. As such, we propose a possible heme-catalyzed mechanism that leads to $ONOO^-$ nitration of the internal Tyr 385 residue that is critical to PGHS-1 activity (**Fig. 9**). In the proposed scheme, catalysis is likely initiated by $ONOO^-$ reaction with Fe^{III} heme, resulting in the formation of a Fe^{III}-ONOO complex (pathway A) and producing the Fe^{IV}=O porphyrin cation radical intermediate and NO_2^-. The Fe^{IV}=O porphyrin cation radical (intermediate I) has been observed during PGHS-1 activation (52). Electron transfer from NO_2^- to the porphyrin cation radical intermediate may occur, resulting in nitrogen dioxide ($^{\bullet}NO_2$) formation (pathway B).

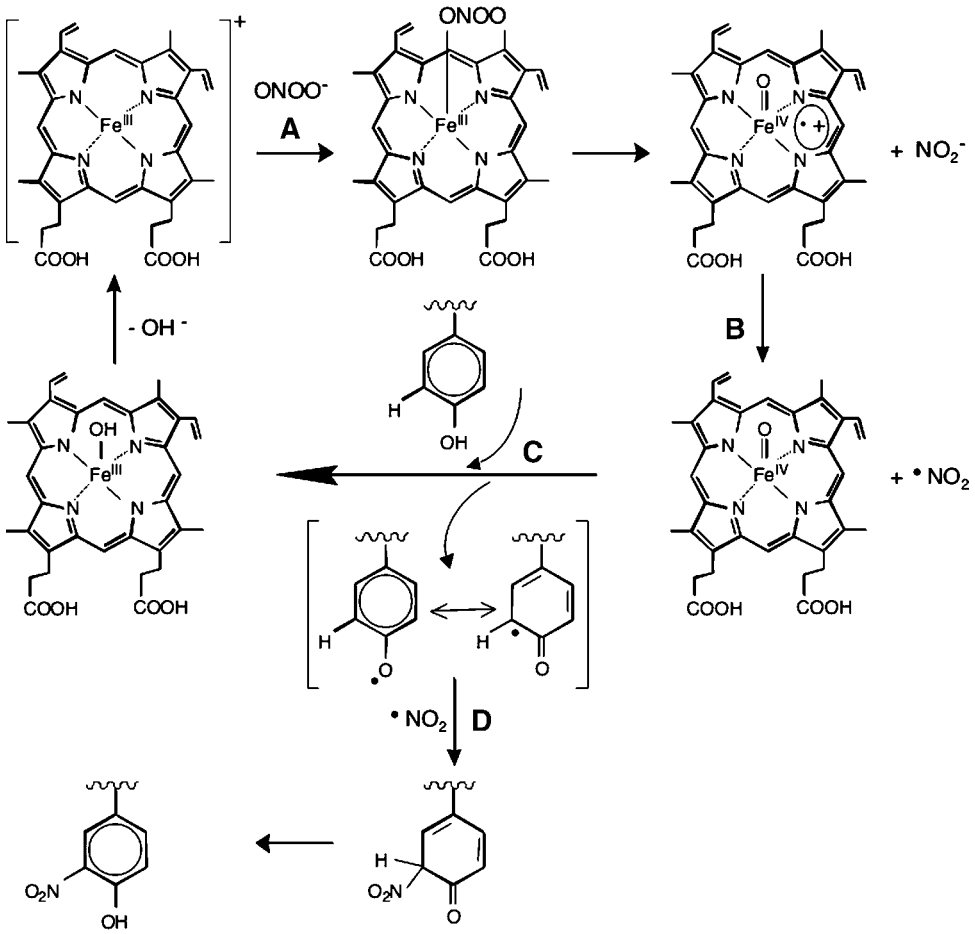

Fig. 9. Proposed mechanism of PGHS-1 Tyr 385 nitration by $ONOO^-$. Reaction A: $ONOO^-$ oxidizes the Fe^{III} heme to a Fe^{IV}=O porphyrin cation radical and NO_2^- via a Fe^{III}-ONOO intermediate. Reaction B: Electron transfer from NO_2^- to the porphyrin cation radical intermediate and formation of nitrogen dioxide ($^{\bullet}NO_2$). Reaction C: Hydrogen atom transfer from Tyr 385 leading to Tyr radical formation. Reaction D: Coupling of the Tyr radical and $^{\bullet}NO_2$ to form 3-nitrotyrosine.

Hydrogen atom abstraction from Tyr 385 (pathway C) results in a Tyr radical that can couple with $^{\bullet}NO_2$ to form 3-nitrotyrosine (pathway D).

Another potentially important observation (Fig. 8) is that the heme group catalyzes PGHS-1 multimer formation in the presence of $ONOO^-$. The mechanism of aggregation is unknown. However, we can rule out the contribution of disulfide formation, because samples used in Western blot analysis were treated with a potent thiol reductant (mercaptoethanol). An alternative process leading to multimer formation could involve dityrosine cross-linking, which has been observed in proteins identified in neurodegenerative disorders (53). Multimer formation was increased by arachidonic acid via mechanisms that await elucidation.

In summary, we show that $ONOO^-$ acts at the peroxidase site of PGHS-1 to inactivate catalytic function. This reaction initially activates the peroxidase site of PGHS-1 but subsequently yields modified forms of PGHS-1, which are catalytically incompetent. These modifications involve perturbations to the PGHS-1 backbone and heme absorption characteristics, Tyr nitration, and multimer formation. The levels of Tyr nitration and multimer formation are modulated by arachidonic acid and heme. Nitration, however, had no impact on the ability of apoPGHS-1 to reconstitute heme and metabolize arachidonic acid. Heme serves to target nitration to the critical Tyr 385 residue, increasing overall Tyr nitration and multimer formation in holoPGHS-1 compared with apoPGHS-1. We propose that heme plays a decisive role in catalyzing these processes in PGHS-1 and potentially other hemoproteins that become exposed to nitrative stress in an inflammatory setting.

The authors are particularly grateful to Drs. Domenick Falcone and Esther Breslow for helpful discussions during the course of this study. Drs. Gerard Parkin, Andrew Nicholson, and Rosemary Kraemer are thanked for helpful suggestions. The authors acknowledge Dr. Mike Hare of the Mass Spectrometry Facilities and Services Core at the Oregon State University Environmental Health Sciences Center. The authors are indebted to Ms. Barbara Summers for expert technical help. This study was supported, in part, by National Institutes of Health Grants HL-46403 and HL-07423 and National Institutes of Health Training Grant T-32 HL-07423 to D.P.H., by National Institutes of Health Grants HL-46403, HL-50656, and RR-19355 to S.S.G., by an Atorvastatin Research Award (Pfizer, Inc.) to R.S.D., by a Philip Morris USA, Inc., and Philip Morris International grant awarded to R.K.U., by National Science Foundation Career Grant MCB-0417181 to E.J.B., by National Institutes of Health Grant P30 ES-00210 to the Oregon State University Environmental Health Sciences Center, and by the Abercrombie Foundation.

REFERENCES

1. Dusting, G. J., S. Moncada, and J. R. Vane. 1977. Prostacyclin (PGX) is the endogenous metabolite responsible for relaxation of coronary arteries induced by arachidonic acid. *Prostaglandins.* **13:** 3–15.
2. Davidge, S. T. 2001. Prostaglandin H synthase and vascular function. *Circ. Res.* **89:** 650–660.
3. Marnett, L. J. 1990. Prostaglandin synthase-mediated metabolism of carcinogens and a potential role for peroxyl radicals as reactive intermediates. *Environ. Health Perspect.* **88:** 5–12.
4. Hla, T., A. Ristimaki, S. Appleby, and J. G. Barriocanal. 1993. Cyclooxygenase gene expression in inflammation and angiogenesis. *Ann. N. Y. Acad. Sci.* **696:** 197–204.
5. Picot, D., P. J. Loll, and R. M. Garavito. 1994. The X-ray crystal structure of the membrane protein prostaglandin H2 synthase-1. *Nature.* **367:** 243–249.
6. Dietz, R., W. Nastainczyk, and H. H. Ruf. 1988. Higher oxidation states of prostaglandin H synthase. Rapid electronic spectroscopy detected two spectral intermediates during the peroxidase reaction with prostaglandin G2. *Eur. J. Biochem.* **171:** 321–328.
7. Smith, W. L., and L. J. Marnett. 1991. Prostaglandin endoperoxide synthase: structure and catalysis. *Biochim. Biophys. Acta.* **1083:** 1–17.
8. Tsai, A. L., G. Palmer, and R. J. Kulmacz. 1992. Prostaglandin H synthase. Kinetics of tyrosyl radical formation and of cyclooxygenase catalysis. *J. Biol. Chem.* **267:** 17753–17759.
9. Smith, W. L., and W. E. M. Lands. 1972. Oxygenation of polyunsaturated fatty acids during prostaglandin biosynthesis by sheep vesicular glands. *Biochemistry.* **11:** 3276–3285.
10. Teruhiko, S., R. J. Kulmacz, D. L. DeWitt, and W. L. Smith. 1990. Tyrosine 385 of prostaglandin endoperoxide synthase is required for cyclooxygenase catalysis. *J. Biol. Chem.* **265:** 20073–20076.
11. Hsi, L. C., C. W. Hoganson, G. T. Babcock, R. M. Garavito, and W. L. Smith. 1995. An examination of the source of the tyrosyl radical in ovine prostaglandin endoperoxide synthase-1. *Biochem. Biophys. Res. Commun.* **207:** 652–660.
12. Shi, W., C. W. Hoganson, M. Espe, C. J. Bender, G. T. Babcock, G. Palmer, R. J. Kulmacz, and A-L. Tsai. 2000. Electron paramagnetic resonance and electron nuclear double resonance spectroscopic identification and characterization of the tyrosyl radicals in prostaglandin H synthase-1. *Biochemistry.* **39:** 4112–4121.
13. Salvemini, D., S. L. Settle, J. L. Masferrer, K. Seibert, M. G. Currie, and P. Needleman. 1995. Regulation of prostaglandin production by nitric oxide: an in vivo analysis. *Br. J. Pharmacol.* **114:** 1171–1178.
14. Marnett, L. J., T. L. Wright, B. C. Crews, S. R. Tannenbaum, and J. D. Morrow. 2000. Regulation of prostaglandin biosynthesis by nitric oxide is revealed by targeted deletion of inducible nitric-oxide synthase. *J. Biol. Chem.* **275:** 13427–13430.
15. Upmacis, R. K., R. S. Deeb, and D. P. Hajjar. 1999. Regulation of prostaglandin H2 synthase activity by nitrogen oxides. *Biochemistry.* **38:** 12505–12513.
16. Salvemini, D., T. P. Misko, J. L. Masferrer, K. Seibert, M. G. Currie, and P. Needleman. 1993. Nitric oxide activates cyclooxygenase enzymes. *Proc. Natl. Acad. Sci. USA.* **90:** 7240–7244.
17. Landino, L. M., B. C. Crews, M. D. Timmons, J. D. Morrow, and L. J. Marnett. 1996. Peroxynitrite, the coupling product of nitric oxide and superoxide, activates prostaglandin biosynthesis. *Proc. Natl. Acad. Sci. USA.* **93:** 15069–15074.
18. Kim, S. F., D. A. Huri, and S. H. Snyder. 2005. Inducible nitric oxide synthase binds, S-nitrosylates, and activates cyclooxygenase-2. *Science.* **310:** 1966–1970.
19. Kanner, J., S. Harel, and R. Granit. 1992. Nitric oxide, an inhibitor of lipid oxidation by lipoxygenase, cyclooxygenase and hemoglobin. *Lipids.* **27:** 46–49.
20. Stamler, J. S., D. J. Singel, and J. Loscalzo. 1992. Biochemistry of nitric oxide and its redox-activated forms. *Science.* **258:** 1898–1902.
21. Radi, R., A. Denicola, and B. A. Freeman. 1999. Peroxynitrite reactions with carbon dioxide-bicarbonate. *Methods Enzymol.* **301:** 353–367.
22. Lymar, S. V., Q. Jiang, and J. K. Hurst. 1996. Mechanism of carbon dioxide-catalyzed oxidation of tyrosine by peroxynitrite. *Biochemistry.* **35:** 7855–7861.
23. Upmacis, R. K., R. S. Deeb, M. J. Resnick, R. Lindenbaum, C. Gamss, D. Mittar, and D. P. Hajjar. 2004. Involvement of mitogen-activated protein kinase cascade in peroxynitrite-mediated arachidonic acid release in vascular smooth muscle cells. *Am. J. Physiol. Cell Physiol.* **286:** C1271–C1280.
24. Deeb, R. S., M. J. Resnick, D. Mittar, T. McCaffrey, D. P. Hajjar, and R. K. Upmacis. 2002. Tyrosine nitration in prostaglandin H2 synthase. *J. Lipid Res.* **43:** 1718–1726.
25. Boulos, C., H. Jiang, and M. Balazy. 2000. Diffusion of peroxynitrite into the human platelet inhibits cyclooxygenase via nitration of tyrosine residues. *J. Pharmacol. Exp. Ther.* **293:** 222–229.
26. Kulmacz, R. J., Y. Ren, A-L. Tsai, and G. Palmer. 1990. Pros-

taglandin H synthase: spectroscopic studies of the interaction with hydroperoxides and with indomethecin. *Biochemistry.* **29:** 8760–8771.
27. Goodwin, D. C., M. R. Gunther, L. C. Hsi, B. C. Crews, T. E. Eling, R. P. Mason, and L. J. Marnett. 1998. Nitric oxide trapping of tyrosyl radicals generated during prostaglandin endoperoxide synthase turnover. Detection of the radical derivative of tyrosine 385. *J. Biol. Chem.* **273:** 8903–8909.
28. Shimokawa, T., R. J. Kulmacz, D. L. De Witt, and W. L. Smith. 1990. Tyrosine 385 of prostaglandin endoperoxide synthase is required for cyclooxygenase catalysis. *J. Biol. Chem.* **265:** 20073–20076.
29. Van der Ouderaa, F. J., M. Buytenhek, D. H. Nugteren, and D. A. Van Dorp. 1977. Purification and characterisation of prostaglandin endoperoxide synthetase from sheep vesicular glands. *Biochim. Biophys. Acta.* **487:** 315–331.
30. Malkowski, M. G., M. J. Theisen, A. Scharmen, and M. R. Garavito. 2000. The formation of stable fatty acid substrate complexes in prostaglandin H_2 synthase-1. *Arch. Biochem. Biophys.* **380:** 39–45.
31. Tsai, A-L., R. J. Kulmacz, J. S. Wang, Y. Wang, H. E. Van Wart, and G. Palmer. 1993. Heme coordination of prostaglandin H synthase. *J. Biol. Chem.* **268:** 8554–8563.
32. Wu, G., J. L. Vuletich, R. J. Kulmacz, Y. Osawa, and A-L. Tsai. 2001. Peroxidase self-inactivation in prostaglandin H synthase-1 pretreated with cyclooxygenase inhibitors or substituted with mangano protoporphyrin IX. *J. Biol. Chem.* **276:** 19879–19888.
33. Loll, P. J., C. T. Sharkey, S. J. O'Connor, C. M. Dooley, E. O'Brien, M. Devocelle, K. B. Nolan, B. S. Selinsky, and D. J. Fitzgerald. 2001. O-Acetylsalicylhydroxamic acid, a novel acetylating inhibitor of prostaglandin H_2 synthase: structural and functional characterization of enzyme-inhibitor interactions. *Mol. Pharmacol.* **60:** 1407–1413.
34. Kulmacz, R. J. 1987. Prostaglandin G_2 levels during reaction of prostaglandin H synthase with arachidonic acid. *Prostaglandins.* **34:** 225–240.
35. Garavito, M. R., and D. Picot. 1990. The art of crystallizing membrane proteins. *Methods: A Companion to Methods in Enzymology.* **1:** 57–69.
36. Jones, B. L. 2001. Interactions of malt and barley (*Hordeum vulgare* L.) endoproteinases with their endogenous inhibitors. *J. Agric. Food Chem.* **49:** 5975–5981.
37. Hogg, N., V. M. Darley-Usmar, M. T. Wilson, and S. Moncada. 1992. Production of hydroxyl radicals from the simultaneous generation of superoxide and nitric oxide. *Biochem. J.* **281:** 419–424.
38. Carmichael, A. J., L. Steel-Goodwin, B. Gray, and C. M. Arroyo. 1993. Reactions of active oxygen and nitrogen species studied by EPR and spin trapping. *Free Radic. Res. Commun.* **19 (suppl.):** S1–S16.
39. Rodriguez, A. A., K. A. Grunberg, and E. L. Taleisnik. 2002. Reactive oxygen species in the elongation zone of maize leaves are necessary for leaf extension. *Plant Physiol.* **129:** 1627–1632.
40. Rehman, A., M. Whiteman, and B. Halliwell. 1997. Scavenging of hydroxyl radicals but not of peroxynitrite by inhibitors and substrates of nitric oxide synthases. *Br. J. Pharmacol.* **122:** 1702–1706.
41. Cohen, I. A. 1969. The dimeric nature of hemin hydroxides. *J. Am. Chem. Soc.* **91:** 1980–1983.
42. Koppenol, W. H. 1998. The basic chemistry of nitrogen monoxide and peroxynitrite. *Free Radic. Biol. Med.* **25:** 385–391.
43. Huie, R. E., and S. Padmaja. 1993. The reaction of NO with superoxide. *Free Radic. Res. Commun.* **18:** 195–199.
44. Radi, R., J. S. Beckman, K. M. Bush, and B. A. Freeman. 1991. Peroxynitrite oxidation of sulfhydryls. The cytotoxic potential of superoxide and nitric oxide. *J. Biol. Chem.* **266:** 4244–4250.
45. Kennedy, T. A., C. J. Smith, and L. J. Marnett. 1994. Investigation of the role of cysteines in catalysis by prostaglandin endoperoxide synthase. *J. Biol. Chem.* **269:** 27357–27364.
46. Upmacis, R. K., D. P. Hajjar, B. T. Chait, and U. A. Mirza. 1997. Direct observation of nitrosylated heme in myoglobin and hemoglobin by electrospray ionization mass spectrometry. *J. Am. Chem. Soc.* **119:** 10424–10429.
47. Balazy, M., P. M. Kaminski, K. Mao, J. Tan, and M. S. Wolin. 1998. S-Nitroglutathione, a product of the reaction between peroxynitrite and glutathione that generates nitric oxide. *J. Biol. Chem.* **273:** 32009–32015.
48. Marshall, P. J., R. J. Kulmacz, and W. E. Lands. 1987. Constraints on prostaglandin biosynthesis in tissues. *J. Biol. Chem.* **262:** 3510–3517.
49. Sies, H., V. S. Sharov, L. O. Klotz, and K. Briviba. 1997. Glutathione peroxidase protects against peroxynitrite-mediated oxidations. A new function for selenoproteins as peroxynitrite reductase. *J. Biol. Chem.* **272:** 27812–27817.
50. Pietraforte, D., A. M. Salzano, G. Scorza, G. Marino, and M. Minnetti. 2001. Mechanism of peroxynitrite interaction with ferric hemoglobin and identification of nitrated tyrosine residues. CO_2 inhibits heme-catalyzed scavenging and isomerization. *Biochemistry.* **40:** 15300–15309.
51. Daiber, A., M. Bachschmid, J. S. Beckman, T. Munzel, and V. Ullrich. 2004. The impact of metal catalysis on protein tyrosine nitration by peroxynitrite. *Biochem. Biophys. Res. Commun.* **317:** 873–881.
52. Karthein, R., R. Dietz, W. Nastainczyk, and H. H. Ruf. 1988. Higher oxidation states of prostaglandin H synthase. *Eur. J. Biochem.* **171:** 313–320.
53. Souza, J. M., B. I. Giasson, Q. Chen, V. M-Y. Lee, and H. Ischiropoulos. 2000. Dityrosine cross-linking promotes formation of stable alpha-synuclein polymers. Implication of nitrative and oxidative stress in the pathogenesis of neurodegenerative synucleinopathies. *J. Biol. Chem.* **275:** 18344–18349.